

Ultrathin film, high specific power InP solar cells on flexible plastic substrates

Kuen-Ting Shiu, Jeremy Zimmerman, Hongyu Wang, and Stephen R. Forrest

Citation: *Appl. Phys. Lett.* **95**, 223503 (2009); doi: 10.1063/1.3268805

View online: <http://dx.doi.org/10.1063/1.3268805>

View Table of Contents: <http://apl.aip.org/resource/1/APPLAB/v95/i22>

Published by the [American Institute of Physics](#).

Related Articles

Exploiting piezoelectric charge for high performance graded InGa_N nanowire solar cells

Appl. Phys. Lett. **101**, 143905 (2012)

Design principles for plasmonic thin film GaAs solar cells with high absorption enhancement

J. Appl. Phys. **112**, 054326 (2012)

Optical absorptions in Al_xGa_{1-x}As/GaAs quantum well for solar energy application

J. Appl. Phys. **112**, 054314 (2012)

Analyzing nanotextured transparent conductive oxides for efficient light trapping in silicon thin film solar cells

Appl. Phys. Lett. **101**, 103903 (2012)

Subbandgap current collection through the implementation of a doping superlattice solar cell

Appl. Phys. Lett. **101**, 073901 (2012)

Additional information on *Appl. Phys. Lett.*

Journal Homepage: <http://apl.aip.org/>

Journal Information: http://apl.aip.org/about/about_the_journal

Top downloads: http://apl.aip.org/features/most_downloaded

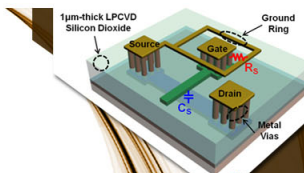
Information for Authors: <http://apl.aip.org/authors>

ADVERTISEMENT



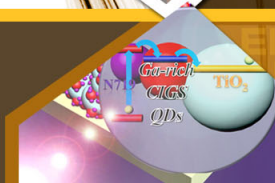
**EXPLORE WHAT'S
NEW IN APL**

SUBMIT YOUR PAPER NOW!



SURFACES AND INTERFACES

Focusing on physical, chemical, biological, structural, optical, magnetic and electrical properties of surfaces and interfaces, and more...



ENERGY CONVERSION AND STORAGE

Focusing on all aspects of static and dynamic energy conversion, energy storage, photovoltaics, solar fuels, batteries, capacitors, thermoelectrics, and more...

Ultrathin film, high specific power InP solar cells on flexible plastic substrates

Kuen-Ting Shiu,^{1,2} Jeramy Zimmerman,² Hongyu Wang,² and Stephen R. Forrest^{2,a)}

¹Department of Electrical Engineering, Princeton University, Princeton, New Jersey 08544, USA

²Department of Electrical Engineering and Computer Science, Material Science and Engineering, and Physics, University of Michigan, Ann Arbor, Michigan 48109, USA

(Received 11 September 2009; accepted 4 November 2009; published online 2 December 2009)

We demonstrate ultrathin-film, single-crystal InP Schottky-type solar cells mounted on flexible plastic substrates. The lightly p-doped InP cell is grown epitaxially on an InP substrate via gas source molecular beam epitaxy. The InP substrate is removed via selective chemical wet-etching after the epitaxial layers are cold-welded to a 25 μm thick Kapton[®] sheet, followed by the deposition of an indium tin oxide top contact that forms the Schottky barrier with InP. The power conversion efficiency under 1 sun is $10.2 \pm 1.0\%$, and its specific power is 2.0 ± 0.2 kW/kg. The ultrathin-film solar cells can tolerate both tensile and compressive stress by bending over a <1 cm radius without damage. © 2009 American Institute of Physics. [doi:10.1063/1.3268805]

For portable, and particularly air and space-borne applications, solar cell power conversion efficiency, radiation resistance, and specific power (kW/kg) must be maximized. Conventional Si and GaAs solar cells have high beginning-of-life efficiency but suffer from performance degradation under irradiation.¹ In contrast, single-crystalline InP is useful in space-borne applications due to its radiation hardness¹ and potentially high power conversion efficiency.^{2,3} However, there have been limited efforts in making thin-film InP solar cells on lightweight substrates that satisfy the demanding requirements for high specific power. Therefore, radiation-resistant copper-indium gallium diselenide (CIGS) (Refs. 4–7) and CdTe (Ref. 8) cells have gradually drawn attention as they are also compatible with growth on thin and lightweight substrates. In this work, we apply the cold-welding^{9,10} technique to bond single-crystal Schottky-type InP ultrathin epitaxial-film solar cells on flexible plastic substrates that can tolerate both tensile and compressive stress by bending around radii as small as 1 cm without damage, obtain a power conversion efficiency of $\eta_p = 10.2 \pm 1.0\%$ and a high specific power of $P_{sp} = 2.0 \pm 0.2$ kW/kg.

The epitaxial solar cell structure is grown by gas source molecular beam epitaxy on a p-type, Zn-doped (100) InP substrate. The epitaxial structure consists of a 0.375 μm thick, p-type ($5 \times 10^{16} \text{ cm}^{-3}$) InP buffer layer, a 0.25 μm thick, lattice-matched Be-doped ($5 \times 10^{16} \text{ cm}^{-3}$) p-type $\text{In}_{0.53}\text{Ga}_{0.47}\text{As}$ etch-stop layer, a 2.0 μm thick, lightly p-doped ($5 \times 10^{16} \text{ cm}^{-3}$) InP absorption layer, and finally, a 0.3 μm thick, lattice-matched Be-doped ($1 \times 10^{19} \text{ cm}^{-3}$) p-type InP ohmic contact layer.

The fabrication of the solar cells starts with electron-beam evaporation of the p-metal contact with thickness of 300 Å Pt followed by 300 Å Au on both the top InP contact layer and the 25 μm thick Kapton sheet. After metal deposition, the wafer is mounted metal-side down on the Pt/Au-coated plastic sheet. A bond is formed between the two metal surfaces via cold-welding^{9,10} by applying a pressure of 50 MPa for 60 s using an MTS Alliance RT/100 Testing System.

The InP substrate and the subsequent $\text{In}_{0.53}\text{Ga}_{0.47}\text{As}$ etch-stop layer are then removed using a $\text{H}_3\text{PO}_4:\text{HCl}=1:3$ solution, followed by $\text{H}_2\text{SO}_4:\text{H}_2\text{O}_2:\text{H}_2\text{O}=1:1:10$. The etch rates for these solutions are 3 $\mu\text{m}/\text{min}$ for InP and 0.2 $\mu\text{m}/\text{min}$ for $\text{In}_{0.53}\text{Ga}_{0.47}\text{As}$, respectively. Finally, a 150 nm thick indium-tin-oxide (ITO) Schottky diode contact with the area of 0.785 mm^2 defined by a shadow mask is sputtered at a base pressure of 2×10^{-6} torr, RF power of 40 W, and deposition rate of 0.2 Å/sec. The sputtered ITO film typically has a resistivity of $\sim 1 \times 10^{-2} \Omega \text{ cm}$ and a transmission coefficient of $\sim 80\%$ to wavelengths in the range of $400 \text{ nm} < \lambda < 900 \text{ nm}$.^{3,11} A control ITO/InP solar cell with a structure similar to the thin-film device was similarly fabricated without substrate removal. The current density (J) versus voltage (V) characteristics were measured in the dark and under simulated illumination from an Oriel AM1.5G solar simulator, using HP4155B semiconductor parameter analyzer. The illumination intensity of the solar simulator was calibrated using a National Renewable Energy Laboratory calibrated silicon reference solar cell. The external quantum efficiency (EQE) measurement was conducted by using a monochromator, an SRS830 lock-in amplifier, and a tungsten lamp. The illumination from tungsten lamp is calibrated with a National Institute of Standards and Technology traceable silicon photodetector.

Figure 1 shows the room temperature J - V characteristics of both thin-film and control photovoltaic cells under simulated AM1.5G solar spectrum at 1 sun intensity ($100 \text{ mW}/\text{cm}^2$). From the dark J - V characteristics of the thin-film device (not shown here), the ideality factor and Schottky barrier height of the thin film solar cell are estimated to be $n=1.14$ and $\phi_B=0.93$ eV respectively by applying the theoretical Richardson constant of p-InP. The specific series resistance and specific shunt resistance of the thin-film device are $5.4 \Omega \text{ cm}^2$ and $3.8 \times 10^8 \Omega \text{ cm}^2$, respectively. The high specific series resistance originates from the nonoptimized ITO contact, and is primarily responsible for the low fill factor of the solar cell. The short circuit photocurrent density (J_{sc}) for the thin film solar cell is $J_{sc}=30 \pm 3 \text{ mA}/\text{cm}^2$, while for the control, $J_{sc}=24.9 \pm 2.5 \text{ mA}/\text{cm}^2$. Integration of the measured EQE (see

^{a)}Electronic mail: stevefor@umich.edu.

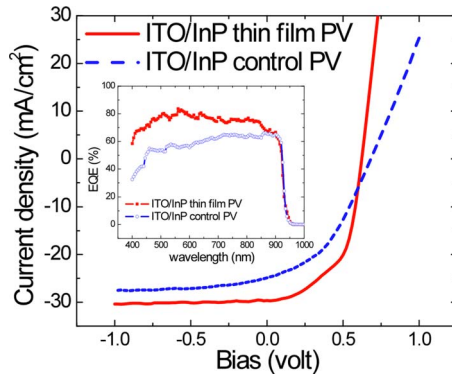


FIG. 1. (Color online) Current density vs voltage characteristics of the ITO/InP thin film and control solar cells under 1 sun, AM1.5G simulated solar illumination. **Inset:** EQE as a function of wavelength of the ITO/InP thin film and control solar cells.

inset, Fig. 1) over the AM1.5 solar spectrum gives $J_{sc} = 25 \pm 3$ and 20 ± 2 mA/cm² for the thin-film and control cells, respectively, consistent with values obtained using simulated solar illumination.

Figures 2(a) and 2(b) show the V_{oc} , fill factor, J_{sc} , and η_p of the ITO/InP thin-film and control solar cells, respectively, as functions of simulated illumination intensity. The V_{oc} of the control solar cell is linearly proportional to the logarithm of the optical intensity, as expected for an intensity-independent responsivity. However, the thin-film solar cell V_{oc} is pinned for illumination intensities >0.5 suns. The exact reason needs to be further investigated but the pinned V_{oc} indicates that the thin-film devices suffer more carrier recombination, most likely due to the surface states from both the front ITO contact and the back metal contact, as the illumination level increases. The fill factor of both devices decreases at high solar intensity because of the high specific series resistance. The lower shunt specific resistance of the control device further decreases the fill factor. Consequently,

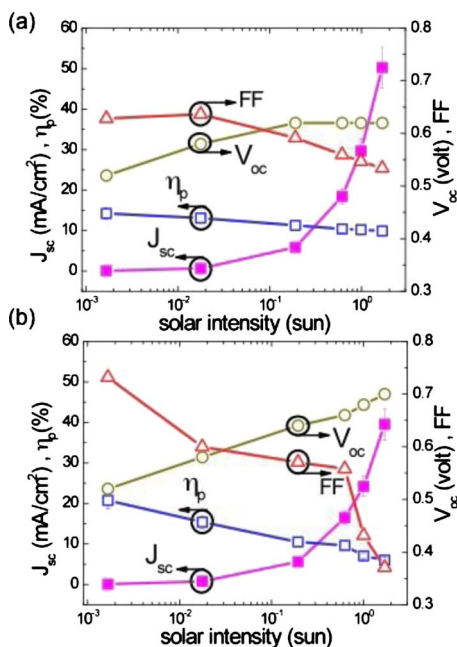


FIG. 2. (Color online) Open circuit voltage (V_{oc}), fill factor (FF), short circuit current (J_{sc}), and power conversion efficiency (η_p) as functions of illumination intensity under a AM1.5G simulated solar spectrum of the (a) thin film ITO/InP (b) control solar cell.

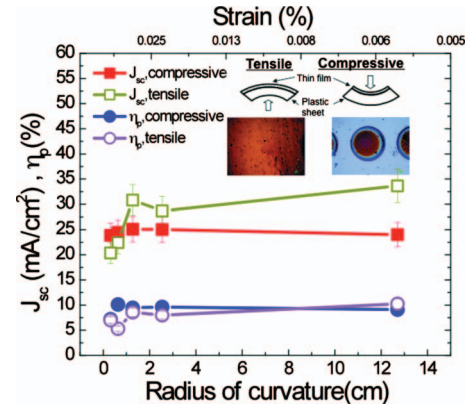


FIG. 3. (Color) Short circuit current (J_{sc}) and power conversion efficiency (η_p) of the thin film ITO/InP solar cell after either the compressive (bending inward) or tensile (bending outward) stress test under 1 sun, AM1.5G simulated solar illumination. **Inset:** Diagram of the bending test, and its corresponding microscope images of the epitaxial InP cell after bending over a 0.3 cm radius.

the power efficiency of the thin-film cell at 1 sun is $\eta_p = 10.2 \pm 1.0\%$ while the control has $\eta_p = 7.0 \pm 0.7\%$.

The flexibility of the thin-film solar cells was tested by bending the devices either inward or outward over cylinders of various radii. Inward bending applies compressive strain, while outward bending results in tensile strain to the InP layer (see inset, Fig. 3). For each bending radius, the thin-film solar cell is stressed for 30 s, released, and then characterized. Figure 3 shows J_{sc} and η_p , respectively, following the stress test. Here, η_p remains unchanged for inward bending radii >0.5 cm (compressive strain $\sim -0.097\%$), and for an outward bending radius >1.0 cm (tensile strain $\sim 0.0486\%$). However, once stressed beyond these values, J_{sc} shows a decrease, leading to a concomitant reduction in power conversion efficiency. Figure 3 (inset) shows a microscope image of a failed thin film solar cell after experiencing tensile stress over a 0.3 cm radius. The cell exhibits cracks that are parallel to the cylindrical axis, while the cell subjected to compressive stress shows no obvious damage. Although stress-induced cracks have an adverse impact on the solar cell performance, the stress tolerance of this InP thin film solar cell can be improved by using a thinner plastic sheet as the substrate, or placing the thin film at the neutral stress surface located at the center of a sandwich formed by two identically thin sheets of plastic.¹² Also, we note that ITO itself is brittle and subject to cracking during stress.¹³ It is unclear whether the cracks initiate in the ITO and propagate into the InP, or vice versa.

Since the Kapton[®] has a significantly lower density (~ 1.42 g/cm³) than InP (4.81 g/cm³), the thin-film solar cell is useful for applications where power conversion using lightweight devices is important. Based on the device structure and the measured power efficiency, the specific powers of the thin-film and control ITO/InP solar cells are $P_{sp} = 2.0 \pm 0.2$ and 0.041 ± 0.004 kW/kg, respectively, while CIGS or CdTe thin-film solar cells have reported specific powers of 3.3 (Ref. 6) and 2.0 kW/kg,⁸ respectively. A detailed comparison of this work with other reported thin-film solar cell technologies is provided in Table I. By adopting a thinner plastic substrate and using a higher efficiency solar cell architecture, over double the specific power is anticipated.

TABLE I. Comparison of different thin-film solar cell performances on light-weight substrates. The η_p of the CIGS cell is calculated by assuming that the density of CIGS film is 5.85 g/cm^3 , and the top metal contact consists of a $5 \text{ }\mu\text{m}$ thick Al/Ni stack with 5% device coverage (Ref. 7).

Device structure	ITO/InP	CIGS	CdTe	GaAs thin-film
Substrate	Kapton foil (25 μm thick)	Upilex foil (12.5 μm thick)	Upilex film (10 μm thick)	Glass (75 μm thick)
η_p (%)	10.2 ± 1.0	14.1	11.4	19.2
P_{sp} (kW/kg)	2.0 ± 0.2	3.3	2	1.1
V_{oc} at 1 sun (V)	0.62	0.649	0.765	1.0
J_{sc} at 1 sun (mA/cm^2)	29.6 ± 2.9	31.5	20.9	31.8
Fill factor	0.55	0.69	0.71	0.806
Reference	This work	See Ref. 6	See Ref. 8	See Ref. 14

In conclusion, we have demonstrated ultrathin-film InP Schottky-type solar cells bonded to flexible plastic substrates via cold-welding. The device exhibits a power conversion efficiency of $10.2 \pm 1.0\%$ and a specific power of $2.0 \pm 0.2 \text{ kW/kg}$. The devices are capable of withstanding either compressive or tensile strain by bending over radii of 1.0 cm or greater without degradation. This work provides an alternative method for adopting III–V semiconductor solar cells for portable, air and space-borne applications where very high specific power efficiency is required.

The authors thank the Army Research Laboratory MAST program and Global Photonic Energy Corporation for partial support of this work.

¹I. Weinberg, *Sol. Cells* **29**, 225 (1990).

²C. J. Keavney, V. E. Haven, and S. M. Vernon, 21st IEEE Photovoltaic Specialists Conference, Proc., 141 (1990).

³T. J. Coutts and S. Naseem, *Appl. Phys. Lett.* **46**, 164 (1985).

⁴K. Otte, L. Makhova, A. Braun, and I. Konovalov, *Thin Solid Films* **511**, 613 (2006).

⁵D. C. Senft, *J. Electron. Mater.* **34**, 1099 (2005).

⁶D. Bremaud, D. Rudmann, G. Bilger, H. Zogg, and A. N. Tiwari, 31st IEEE Photovoltaic Specialists Conference, Proc., 223 (2005).

⁷J. R. Tuttle, A. Szalaj, and J. Keane, 28th IEEE Photovoltaic Specialists Conference, Proc., 1042 (2000).

⁸A. Romeo, G. Khrypunov, F. Kurdesau, M. Arnold, D. L. Bätzner, H. Zogg, and A. N. Tiwari, *Sol. Energy Mater. Sol. Cells* **90**, 3407 (2006).

⁹C. Kim, P. Burrows, and S. R. Forrest, *Science* **288**, 831 (2000).

¹⁰G. S. Ferguson, M. K. Chaudhury, G. B. Sigal, and G. M. Whitesides, *Science* **253**, 776 (1991).

¹¹K. Carl, H. Schmitt, and I. Friedrich, *Thin Solid Films* **295**, 151 (1997).

¹²Z. Suo, E. Y. Ma, H. Gleskova, and S. Wagner, *Appl. Phys. Lett.* **74**, 1177 (1999).

¹³Y. Leterrier, L. Medico, F. Demarco, J.-A. E. Manson, U. Betz, M. F. Escola, M. Kharrazi Olsson, and F. Atamny, *Thin Solid Films* **460**, 156 (2004).

¹⁴M. H. Hannon, M. W. Dashiell, L. C. DiNetta, and A. M. Barnett, 25th IEEE Photovoltaic Specialists Conference, Proc., 191 (1996).